Contact Elimination in Mechanical Face Seals Using Active Control

Joshua Dayan*, Technion – Israel Institute of Technology, Min Zou+, Seagate Technology, Inc. and Itzhak Green, Georgia Institute of Technology

Abstract-- **Wear and failure of mechanical seals may be critical in certain applications and should be avoided. Large relative misalignment between the seal faces is the most likely cause for intermittent contact and the increased friction that eventually brings failure. Adjustment of the seal clearance is probably the most readily implemented method of reducing the relative misalignment and eliminating seal face contact during operation. This method is demonstrated with the aid of a noncontacting flexibly mounted rotor (FMR) mechanical face seal test rig employing a cascade control scheme. Eddy current proximity probes measure the seal clearance directly. The inner loop controls the clearance, maintaining a desired gap by adjusting the air pressure in the rotor chamber of the seal. When contact is detected the outer loop adjusts the clearance set point according to variance differences in the probes' signals. These differences in variance have been found to be a reliable quantitative indication for such contacts. They are complimentary to other more qualitative phenomenological indications, and provide the controlled variable data for the outer loop. Experiments are conducted to test and verify this active control scheme and strategy. Analysis and results both show that contrary to intuition for the seal under investigation, reducing seal clearance can eliminate contact, and the outer cascade loop indeed drives the control toward this solution.**

Index terms—**mechanical face seal, clearance control, contact elimination**

1. INTRODUCTION

Mechanical seals are widely used in pumps, compressors, turbomachinery and powered vessels. Two types are employed, contacting and noncontacting mechanical face seals. The first seal type provides the most effective separation of the fluids on both sides of the seal, doing so at the expense of high friction and faster wear. The second type provides longer life but at the cost of some leakage. Premature failure of the seal may inflict damage far exceeding the value of the seal itself and, therefore, it should be avoided. In noncontacting seals the cause of failure is not always clear and may be attributed to the process, operation, design or their combination. Nevertheless, a most probable cause of noncontacting seal failure is the occurrence of some undesired intermittent contact between the seal faces. Therefore, contact elimination is of prime importance, especially in critical applications (such as nuclear reactor cooling pumps) where seal failure may have severe implications.

A comprehensive design that takes into account all the information such as seal face geometry, materials, heat transfer, mechanics, system dynamics and empirical data, promotes long seal life. This, however, is by no means an easy task, and in many cases a great amount of the information is missing. The problem may be tackled though, through active control of the seal operation. This approach has been taken by [1] – [4]. All these researchers concentrated solely on clearance adjustment through temperature control, where temperatures measured by thermocouples were used as the feedback. Temperature increase has been claimed to be the result of friction caused by contact. However, temperature may vary as a result of other physical phenomena or changes in operating conditions. Particularly, when seal faces contact because of large relative misalignments the temperature could still remain low because of the cooling effect of excessive leakage. In addition, thermocouples only measure local sealing dam temperatures, where their location is not necessarily right at the location of contact. Thermal inertia must also be taken into account to anticipate the time delays between event occurrence and control activation. On the whole, temperature measurement is not a direct measurement of the clearance and, therefore, an approach that counts on it may not detect situations of damaging, i.e., contacting seal operation.

In this research, various ways of reducing the relative misalignment and diminishing the possibility of seal face contact are introduced and considered. First contact is monitored from the dynamic behavior of the seal using eddy current proximity probes. These provide instantaneous information on proper or improper seal behavior. Then, a control strategy as well as control system are developed and physically implemented to keep both the clearance and the relative misalignment as small as possible in order to ensure noncontacting operation of the FMR mechanical face seal.

Authors information: *Faculty of Mechanical Engineering, Technion – Israel Institute of Technology, Haifa 32000, Israel

+Seagate Technology, Inc., Minneapolis MN

The George W. Woodruff School of Mechanical Engineering, Georgia Institute of Technology, Atlanta, Georgia 30332-0405.

2. INTERMITTENT FACE CONTACT

A basic description and nomenclature of the FMR mechanical face seal are given in Fig. 1 (see [5] for details of this kinematical model). The sealing dam is the area between the slanted face of the rotor and the fixed stator (both are shown also in Fig. 2). To minimize wear one of these faces is usually made of a softer material, e.g., carbon-graphite. During operation the faces lift off to a certain a centerline clearance, *C,* while the softer material also distorts because of mechanical and thermal deformations, as represented by the coning angle, β^*. Note that both *C,* and β^* are very small (of the order of a micron and mrad, respectively) and, hence, Fig. 1 is not shown to scale for these dimensional parameters. Fluid leakage due to the pressure drop across the seal occurs as fluid flows into the converging gap created by β^* (in Fig. 1 flow occurs from the peripheral area towards the center). Ideally, seal faces are arranged perpendicular to the shaft and parallel to each other. As the name implies, there should be no face contact during the operation of the noncontacting mechanical face seal. However, in reality, during operation contact may occur due to large relative misalignment between the seal faces. The relative misalignment between seal faces, γ^* (see Fig. 1), is the result of manufacturing and assembly tolerances, machine deterioration, or from disturbances in the process operation, bent shafts, etc. Seal face contact, not only generates an impact force that is not easy to predict, it also increases the friction and wear of the faces. Heat generated by prolonged

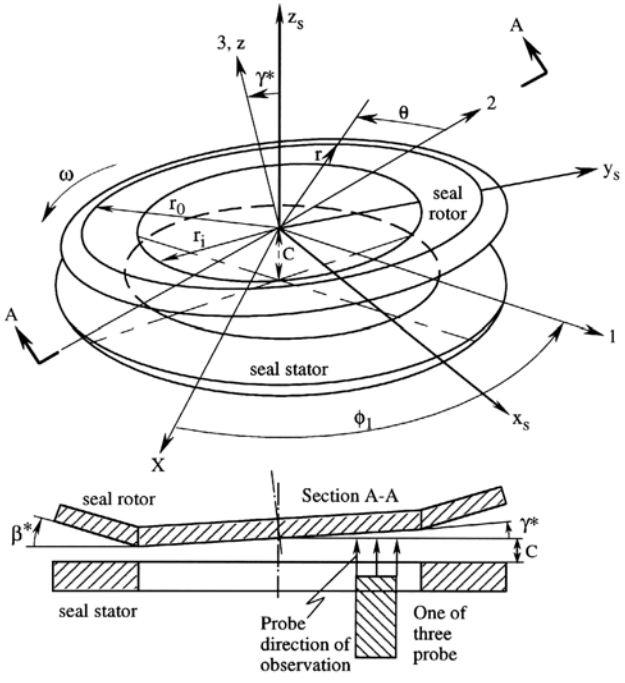

Fig. 1: The relative misalignment between the rotor and the stator in the sealing dam

Whether seal face contact will occur depends not only on the relative misalignment between the rotor and the stator, γ^*, but also on the designed seal clearance, C_o, and the seal inner and outer radii, r_i and r_o (for consistency with previous publications [5 – 15] an asterisk or, a lower-case letter indicates dimensional/non-normalized variables). These can be grouped together into the normalized relative misalignment, γ, defined as $\gamma^* r_o/C_o$ [5]. Seal face contact could either occur at the inner radius or the outer radius, depending on the normalized coning angle, $\beta = \beta^* r_o/C_o$ (now Fig. 1 is better scaled for the nondimensional parameters, where $C = C_o + z_s$). A properly designed seal, must have a coning angle, β, greater than critical [5,8]. (The critical coning angle $\beta_{critical}=1/R_i$, provides positive fluid film stiffness; where R_i is the dimensionless inner radius of the seal, r_i/r_o.) Should contact occur it would take place at the inner radius. In which case, the normalized relative misalignment, γ, can be used to determine contact occurrence. When contact occurs at the inner radius,

$$\gamma^* = C_o / r_i \tag{1}$$

and, therefore, nondimensionally

$$\gamma = 1/R_i = \gamma_{critical} \tag{2}$$

Thus, in order to avoid the possibility of contact between the seal faces both the design and operation should ensure $\gamma < \gamma_{critical}$ at all times.

3. REDUCING THE NORMALIZED RELATIVE MISALIGNMENT

In some applications seal contact can be prevented by proper design, i.e., selecting the seal parameters in such a way that it will not be sensitive to changes in the operational variables about its nominal working point. In other cases, however, the load changes or the disturbances may vary substantially, causing large misalignment, beyond what rigid design can rectify. In the latter one or more of the operational variables, clearance, sealed fluid pressure, and shaft speed, can be used to actively control the seal behavior [6, 7].

The analysis in [5] provides a solution for the dynamic response of the flexibly mounted rotor to two forcing functions: the fixed stator misalignment, and the initial rotor misalignment. Thus, the total rotor misalignment response is the vector superposition of these two responses, and whose maximum is obtained by adding the maxima of the responses to these two forcing function. Likewise, the relative misalignment between the rotor and the stator is the vector subtraction of the total rotor misalignment and the stator misalignment. Hence, reducing the relative misalignment can eliminate contact.

The maximum relative misalignment can be calculated according to the closed form solutions of the Green

dynamic model [5,8]. Based on this solution, parametric and sensitivity studies [6,7,9] were performed to investigate the effect of basic seal parameters (including shaft speed, sealed fluid pressure, coning angle, and clearance) on the maximum relative misalignment for a noncontacting FMR seal test rig (shown in Fig. 2). It was found that increasing the shaft speed and the sealed fluid pressure decreases the maximum normalized relative misalignment. Seal clearance effect on this misalignment, however, depends on the coning angle. This is because of the strong dependence of the rotor dynamic coefficients, and thus the dynamic responses, upon the clearance and coning. Hence, when the coning angle is small, and contrary to intuition, decreasing the seal clearance will decrease the maximum normalized relative misalignment. Conversely when the coning angle is large, increasing the clearance will likewise decrease the maximum normalized relative misalignment. Therefore, the shaft speed, the sealed fluid pressure, or the clearance can be used to reduce the maximum normalized relative misalignment, and eliminate seal face contact. However, since in most applications the shaft speed and sealed fluid pressure are fixed, the best way of contact elimination is by controlling the seal clearance. The present study describes contact elimination by clearance control in a noncontacting FMR seal test rig.

4. CONTACT ELIMINATION

a. The test rig

The basic noncontacting FMR mechanical face seal test rig used in this study (Fig. 2) was described by Lee and Green [10,11,12]. Recently, it has been augmented with an advanced real-time data acquisition and analysis system [13, 14]. Other significant modifications to the basic system include the stator, which is made entirely of carbon graphite, and the rotor, which is made entirely of AISI 440C stainless steel. Both have been fabricated and lapped to industry standards by seal manufacturers (which is better than half a "helium band" or 0.25 μm). The integrated system provides reliable measurement and determination of the relative position between rotor and stator.

The rotor is flexibly mounted on the rotating shaft through an elastomer O-ring. This allows the rotor to track the stator misalignment and to move axially. The seal stator assembly is composed of several components: the carbon stator, the spacer, and the stator holders. This design is capable of mechanically deforming the stator and produces seals with various coning angles [11]. For stability, it is mandatory for the seal to maintain a converging gap in the direction of radial flow. For an outside pressurized seal the minimum seal film thickness has to be on the inside diameter [15]. In real applications the actual coning angle results from pressure differences and thermal stresses. Therefore, it varies over time. However, these transients in deformations occur at a much slower pace than the time scale of interest in seal dynamics. Thus, the two processes (coning angle variations and instantaneous dynamics) can be regarded as decoupled. For this reason the coning in the present test rig is induced by deforming the faces in the stator fixture and held fixed throughout the experiments. In that regard, data sufficient for dynamic analysis and monitoring is acquired in a fraction of a second, a time scale insignificant for any thermal deformations to occur.

The stator assembly is fixed in the housing, which is made of three parts for convenience in machining, maintenance and adjustment of the test rig. All possible leakage paths are sealed by O-rings. The sealed fluid in the housing is pressurized water. The shaft is connected to a spindle driven by a speed controlled DC motor through two pulleys and a timing belt. Pressurized air is supplied from the main air supply line to the rotor chamber through holes in the housing and the shaft. It is sealed by a lip seal at one end and separated from the water by a contacting seal at the other end. The seal operates at an equilibrium clearance where the opening and closing forces are balanced. Changing the closing force by adjusting the air pressure in the rotor chamber (whether manually or by the computer through a voltage to pressure converter) varies the clearance.

Three eddy current proximity probes (REBAM 1200) mounted on the end of the housing measure the instantaneous distances between their tips and the end surface of the rotor face. The eddy current probe sensitivity is 40 $\mu m/V$. The linearity range prevails between 0 - 1 mm. To avoid saturation the proximity probes were located about 0.3 mm from the target rotor surface and the maximum runout was of the order of 10 μm. Hence, the proximity probes never saturated. The proximity probes can measure both the static and the dynamic distances between their tips and the rotor. The three probes are mounted on a circle of 25 mm diameter and located 90° apart. At any particular moment the clearance of the seal is the difference between the instantaneous average readings of the two probes, which are mounted 180° apart, and the zero reference. The latter is obtained once, while the shaft is stationary and high air pressure is applied in the rotor chamber to ensure that the rotor is pressed against the stator. At this state the average of these two probes represents the zero clearance reference. The proximity probes have a bandwidth of about 10 kHz. A low pass filter with a cut-off frequency of 1 kHz is used to eliminate high frequency cross-talk noise among the probes and also to serve as an anti-aliasing filter. The proximity probe signals in terms of the reduced voltages are sent through analog to digital converters to a floating-point Digital Signal Processor (DSP). This DSP, supplemented by a set of on-board peripherals, such as analog to digital and digital to analog converters, comprise a universal board mounted in a personal computer. Since the highest sampling rate of the DSP is 500 kHz, the DSP computational results are available in real-time. It should be mentioned that although

Sehnal, et al. [16], and Etsion and Constantinescu [17], have made similar attempts to determine the clearance from proximity probe readings, they eventually reverted to estimating the clearance indirectly from a simplified equation applied to the measured leakage because of the zero drift resulted from their high operating temperature test conditions

Other key parameters including stator misalignment, rotor misalignment, relative misalignment between the rotor and the stator are calculated on-line in real-time from the probe measurements [13]. Further details of the test rig components, data acquisition and analysis can be found in the aforementioned references.

b. Contact detection and contact elimination strategy

An eigenvalue stability analysis ([5, 8]) reveals that the FMR seal in the current test rig is dynamically stable up to shaft speeds of at least 1300 Hz and below a clearance of 10 μm. These limits are extremely high, and out of the range of normal operation for most practical cases. The problem of contact that occurs here is the steady-state response to the stator misalignment (or initial conditions). A rotor that poorly tracks the stator and its own initial rotor misalignments, leads to a relative misalignment γ (see Fig. 1), large enough to cause contact. The purpose of the contact elimination strategy is to improve upon the rotor response and reduce γ such that noncontacting operator prevails. However, other factors, such as kinematics of the flexible support and its rotordynamic coefficients uncertainties, machine deterioration, transients in sealed pressure or shaft speed, or unexpected shaft vibration, affect the dynamic behavior of the seal and, hence, the relative position and misalignment between the rotor and the stator. The parametric studies ([6, 7, 9]) explore the effects of various seal parameters on this γ_{max} and provide valuable information concerning seal design and performance prediction. These studies also provide guidelines for contact elimination strategy. The undesirable contact, however, makes the system behave very differently than when noncontacting operation prevails. The contacting operation is much more erratic, contains higher harmonics, and the orbit deviates greatly from circular. This, however, is not an instability phenomenon. Particularly, when intermittent face contact occurs the assumption and analysis of a "noncontacting" seal are invalid. A dynamic analysis, which includes intermittent face contact, is extremely difficult and is not yet available. However, the contact elimination strategy based on the studies mentioned above still remains effective for reducing the relative misalignment between rotor and stator. In Zou et al. [18] it was suggested that when it comes to actual diagnostics a phenomenological approach for contact detection is more appropriate. Indeed, it was shown experimentally that under certain conditions (which have been predicted by the analysis) the probe signals become quite erratic, accompanied by higher harmonic oscillations (HHO). (Similar HHO were observed by Lee and Green [10], during intermittent contact, for which they offered a contact model based on a Fourier series expansion.) Power Spectrum Density (PSD) analysis of the probe signals conclusively detects these HHO, in real time. In addition, the angular misalignment orbit, indicating the magnitude of the misalignment when the rotor is positioned at its instantaneous precession angle, obtained during these experiments is non-circular (see orbit for clearance of 6 μm, when contact occurs, in Fig. 3).

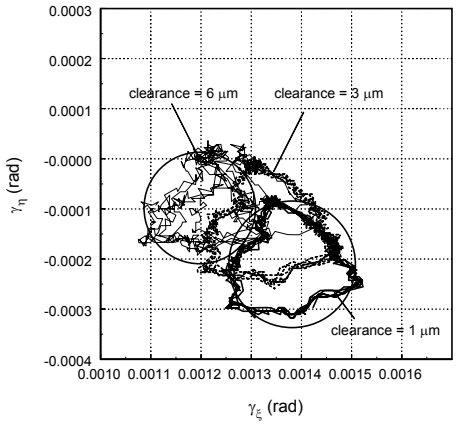

Fig. 3: Rotor angular misalignment orbit (AMO) for different clearances (Large stator and initial rotor misalignments $\gamma_s = \gamma_{ri} = 1.5$ mrad)

The angular misalignment orbit represents the instantaneous locus of two orthogonal tilts γ_ξ and γ_η, which takes place about two inertial coordinates ξ and η (an extensive discussion appears in Green, [5,8], Lee and Green [10] and Zou and Green [13], and the nomenclature in this work is consistent with the definitions in the said references). In summary, because of the factors mentioned above and because the measured clearance oscillates, face contact detection is based on the pattern of the three probe signals, their power spectrum densities and the angular misalignment orbit obtained.

It should be noted that the PSD for all clearances has second higher harmonic oscillations (HHO), which are equal to twice the shaft rotating frequency [18]. Certain levels of these HHO are inherent in the system. They are present even when the rotor runs without the stator in place and are attributed to other system components such as the O-ring flexible support. However, the energy level of these HHO for the contacting case (e.g., the 6 μm clearance case in Fig. 3) is much higher than that of the noncontacting case (1 μm clearance in Fig. 3) and clearly indicates an abnormal operation (i.e., intermittent contact). As seal clearances decrease the shape and peak-to-peak values of the probe signals change as well, and tend to become similar to each other. When the clearance reaches 1 μm

(Fig. 3) the three probe signals are almost identical, and the HHO have practically disappeared. The absence of HHO in the PSD is an indication that noncontacting operation has been restored ([10]) as is the circular orbit obtained [18].

After contact is detected, the required next step should trigger a mechanism, which would dictate the desired clearance to the control loop. Maintaining this desired clearance would eliminate the contact and restore normal (noncontacting) operation.

The contact elimination control system and strategy comprises a nonconventional type of a cascade or supervisory control scheme (Fig. 4). The inner proportional and integral (PI) feedback control loop controls the clearance and maintains a desired set point, which, in turn, is adjusted by the outer control loop. Based on the error between the desired set point and the actual calculated clearance (the mean of three signals obtained from the direct probes measurements) the output signal of the PI algorithm is sent to the electropneumatic transducer (through a D/A converter), which provides the required air pressure to the rotor. As mentioned, the operational conditions are well within the stable region and physically the seal cannot become unstable. Although theoretically the mechanical system is of second order, in reality it behaves more like a first order system having transfer function of $1.07\times10^{-6}(1+0.06s)^{-1}$. With the PI control algorithm ($5\times10^{5}(1+\frac{1}{s})$) tuned by Root Locus consideration) it is possible to maintain any desired clearance value with a high degree of accuracy (e.g., Fig. 5). Zou and Green [14] as well as Zou et al. [18] provide an in-depth description of this part of the control scheme. However, when intermittent (or even persistent) contact occurs, the clearance control loop may still, superficially, show "good" control, i.e., average clearance is maintained at an adequate value, but the contact causes the signal to vibrate (high harmonics appear in the probe signals). In such a case, the outer loop does not look at the mean value of the signal or at any of the individual clearances themselves. Instead, it looks at the high harmonics imposed on the signals whether they correlate (as in noncontacting regime) or not (when contact occurs). After contact is detected, it is corrected or eliminated by dictating a proper clearance to the inner loop. The direction of change in the value of the desired clearance taken by the outer loop is dictated by the sensitivity at the particular coning angle, β, that the seal is operated at (for the test rig clearance decreasing is required).

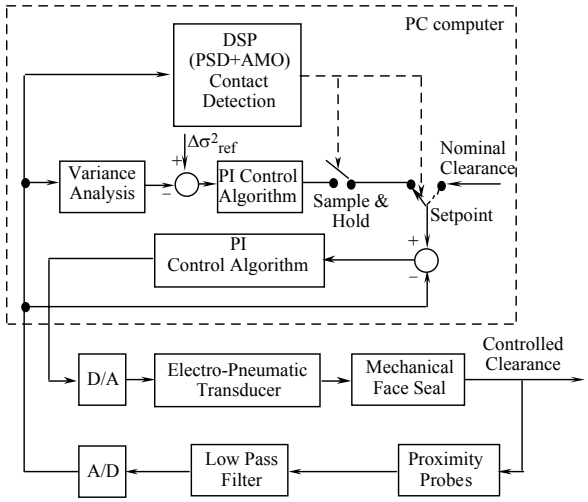

Fig. 4a: Supervisory control using DSP and AMO analysis to detect contact

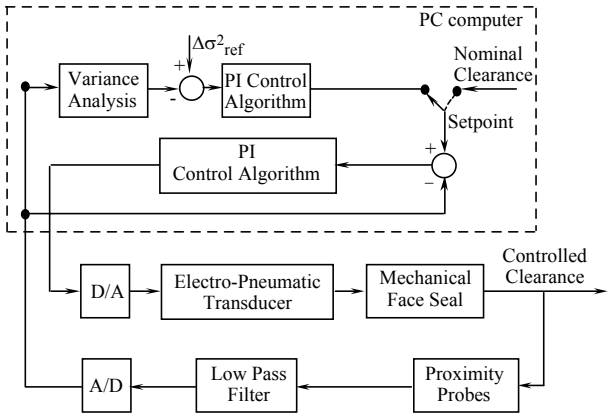

Fig. 4b: Continuous supervisory control using variance analysis to detect contact

Fig. 4: Block diagram of the seal clearance control system

The desired clearance calculations should be based on the statistics of the real-time probe signals and the results of the contact detection test. Since the seal rotor is mounted on the shaft and rotates with the shaft, the signals measured by the three proximity probes should have the same characteristics as long as there is no face contact. In particular, the variance of the probe signals should also be identical and repetitive for any shaft revolution. Therefore, the method suggested here essentially comprises fusing of the clearance measurement data obtained from the three proximity probes. The measurement variance of one probe is compared with those of the other two, and the absolute differences of the variance values are summed and used as feedback to the outer loop.

$$\sum \Delta\sigma_{ij}^{2} = (\sigma_1^2 - \sigma_2^2) + (\sigma_2^2 - \sigma_3^2) + (\sigma_3^2 - \sigma_1^2) \qquad (3)$$

Only the changes in the statistical characteristics (e.g., changes in the variance) of the probe signals other than the

average, and their differences reveal the sought phenomenon.

The contact detection and elimination control may work in two ways:

1. The outer control loop is switched "on" and "off" according to a supervisory algorithm, which determines (by PSD/AMD analysis) whether a contact occurs. When the outer loop is switched off the setpoint for the inner loop is held at its latest updated value (Figure 4a).
2. Alternatively, the outer loop is left "on" all the time (Figure 4b). Practically, this arrangement can eliminate contact with the least control effort.

For the particular experimental rig system in this research and in many similar practical cases, there is essentially no need for "formal" contact detection followed by the initiation of the correcting measures. Instead, the continuous supervisory variance control loop will simply (and reliably) eliminate contacts providing safe operating conditions all the time. The setpoint for the variance was selected to be $\Delta\sigma^2 = 10^{-12}$ m^2, yielding $\Delta\sigma = 10^{-6}$ m, or 50% of the original desired setpoint for the rig (2 μm), i.e., the order of magnitude of face flatness and surface roughness. The variance is calculated for one shaft revolution at sampling interval of 0.0004Sec.

The outer control loop generates the desired clearance output (which is used as the setpoint to the inner control loop). This has been set with a PI algorithm as a smoothing filter and for increasing the overall system accuracy (by zeroing the position error of the outer loop). The employed outer loop controller transfer function for the test rig was $0.5\cdot\left(1+\frac{1}{10\cdot s}\right)$. As indicated, physically, there is no stability limitation for this system and the particular algorithm tuning has been found by trial and error.

The differences in the statistical behavior of the sensor's signals were also used by Shoval et al. [19] for a completely different system, where data fusion from two different sensors measuring location has been used to identify the environment.

c. The clearance control (performance of the inner loop)

As mentioned, seal clearance control (the inner "Slave" loop) is implemented through a PI controller for which the desired value is dictated by the outer "Master" loop. The measured feedback is obtained from the calculated average of the probe signals, and the resulting control action is sent through an electropneumatic transducer that provides the required air pressure in the rotor chamber of the test seal. Various clearances can then be obtained by varying the closing force generated by the air pressure in the rotor chamber.

The ability of the clearance control loop to follow the set-point changes, with and without disturbances in shaft speed and sealed water pressure, is tested and the performance is demonstrated by the test rig. All the experiments are conducted about nominal operation condition of 207 kPa sealed water pressure, 15 Hz shaft rotating speed and 4 μm clearance. The seal coning angle for the experiments is held at 1.6 mrad.

Figure 5 depicts the results of testing the inner control loop for eight minutes. The desired seal clearance (set-point changes), the actually measured clearance and the required air pressure to maintain the set point are plotted. In this test, clearance set-point changes in steps of 25%-50% of the nominal value are introduced along with disturbances in shaft speed (up to 30%) and sealed water pressure (up to 18%). The changes during the test are introduced at one-minute time intervals according to Table 1, where Fig. 5 clearly shows that the controller can follow these set-point changes in the presence of the above-mentioned disturbances. The required control effort, i.e., the air pressure variations in the rotor chamber, seams to be very small.

Table 1: Changes during eight minutes of the test rig control experiment (Fig. 5)

Time	Clearance	Rotation Speed	Sealed water Pressure
Min	μm	Hz	kPa
0	4(*)	15(*)	207(*)
1		20(+5)	
2	3(-1)		
3			241(+34)
4	5(+1)		
5		15	
6			207
7	4		

* Nominal values of the operational conditions
+/- Deviations from the nominal conditions

d. Contact elimination results

Experiments are conducted under different stator coning angles, shaft speeds and sealed water pressures, testing if the entire cascade controller is able to eliminate face contact. The results of one of the experiments (where nominal conditions: β^* = 1.6 mrad, water pressure = 207 kPa, ω = 15 Hz, clearance and stator misalignment 2 mrad, prevail) are plotted in the following set of figures (6-10).

Figure 6 depicts the changes in probe displacement signals obtained when the control is switched on and off. Clearly, the shape and peak-to-peak values of the signals are different for the three probes when control is off, but they are almost identical when the control is on.

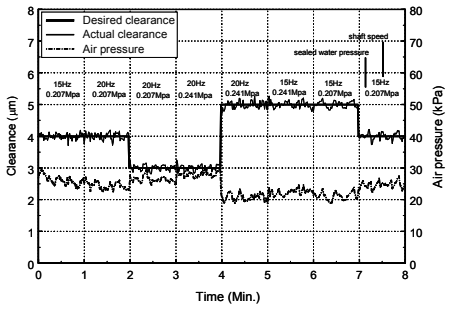

Fig. 5: Transient results with changes according to Table 1

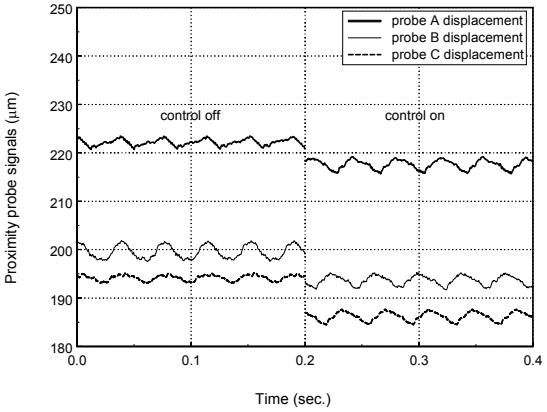

Fig. 6: Proximity probe signals when the control is on and off

It is easier to see these differences from the PSDs of the three probes. The PSD is best presented on a linear scale. On such a scale, control "on" is indicated when the three probes' PSD is 2.5 times higher than the PSD value obtained when the control is "off" at the prime frequency, and it is less than half the value obtained at higher multiplications of this frequency. Because it is impossible to see the differences between the individual PDS of each probe signal on the linear scale the *log*(PSD) is plotted in Fig.7, for the respective control on and control off cases. Although it is less dramatic than the linear plot, Fig. 7 clearly shows that the PSDs of the control "on" match each other much better than those of the control "off".

Fig. 8 shows that the maximum relative misalignment between rotor and stator is significantly reduced when the control is "on" compared to when the control is "off", and hence the two elements are better aligned and contact is less likely (in this case contact is eliminated).
The rotor misalignment orbit for control "on" and control "off" cases, is plotted in Fig. 9. The orbit becomes more circular for the control "on" case, and its center moves towards the point defined by the stator misalignment and angle.

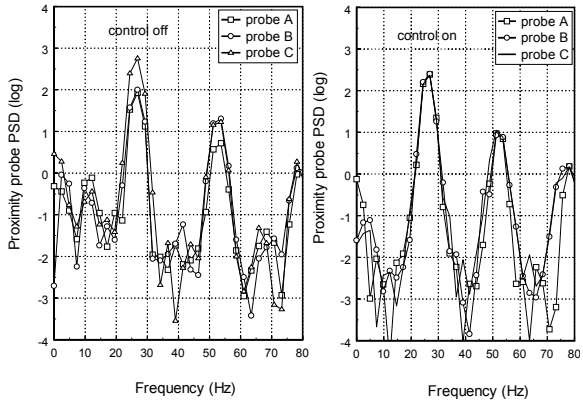

Fig. 7: Proximity probe PSDs when the control is on and off

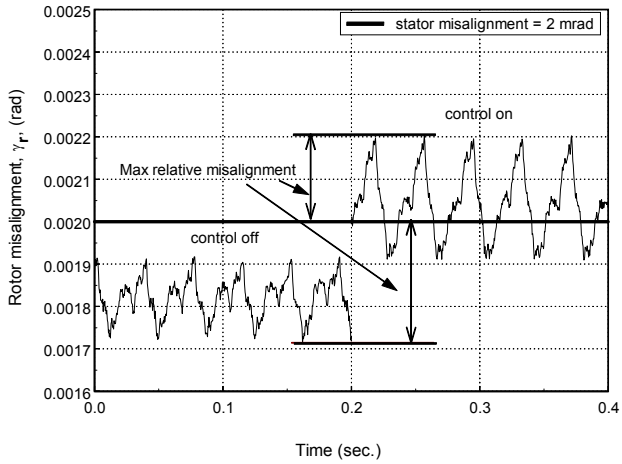

Fig. 8: Rotor misalignment when the control is on and off

When the cascade control is "on," the variance loop drives the system toward better alignment (eliminating the contact), and as can be seen from Fig. 10 it automatically reduces the clearance. This is an indication that under the tested conditions reducing the clearance does indeed reduce the relative misalignment, as was shown analytically by Green [8]. Figure 10 also shows that clearances calculated from the probe measurements are well correlated and in good agreement with clearances calculated from leakage measurements (assuring that both methods are adequate). The changes in the controller output required (the air pressure in the rotor chamber) are very small, demonstrating that the control is well tuned and effective.

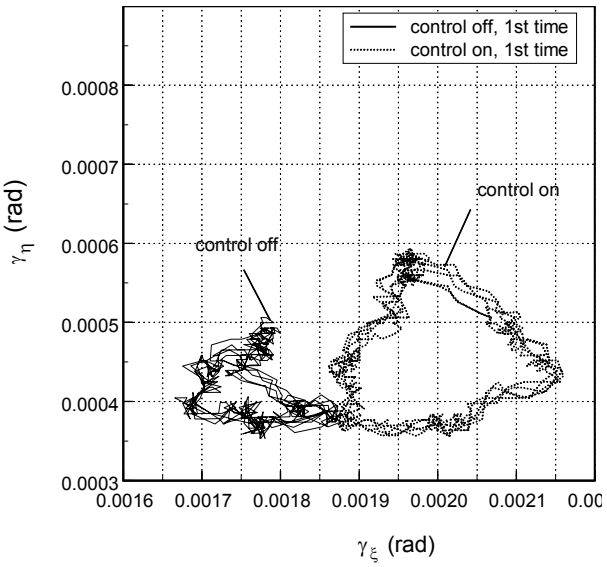

Fig. 9: Rotor angular misalignment orbit for control on and off cases

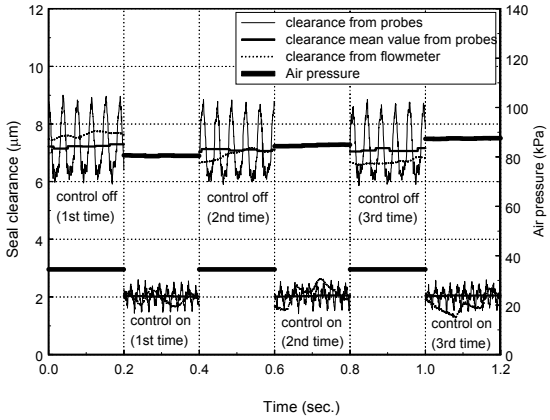

Fig. 10: Seal clearance and air pressure when the control is on and off

5. CONCLUSIONS

A novel method of eliminating contact in mechanical face seals is introduced. This method employs active control of the clearance between the seal faces. It emerged as a conclusion from the results of a detailed parametric and sensitivity analysis for the noncontacting FMR mechanical seal. Contrary to intuition, this work suggests that the clearance should be decreased rather increased, when contact occurs. The reduction in the clearance reduces the relative misalignment between the seal faces; therefore, it reduces the possibility of seal face contact. By bringing the seal faces closer together, not only contact is eliminated, leakage is also significantly reduced.
The active control is realized by a novel cascade scheme using two PI control loops. The inner control loop maintains the desired clearance, while the outer loop calculates and dictates the setpoint, based on the contact detecting result.

The contact is determined by the appearance of abnormal HHO in the signal of the measured clearance (the output of eddy current proximity probes). These HHO are detected by parameters of the DSP and the misalignment orbit for the seal. The novelty of the outer loop is in its reliance on the statistical characteristics of the measured signals and not on the values measured by the sensors. Once the contact has been detected, the outer loop calculates its "feedback" signal by summing the variance differences of the proximity probes signals. It is then compared to the "target" variance – typical behavior of a noncontacting operation – and subsequently determines the new desired gap, which eliminates the contact and resumes normal noncontacting operations. For most practical situations the outer loop can be operated continuously, without the need for separate detection. Deviation from the target variance means appearance of HHO, or the occurrence of a contact, and the outer control loop will take care of this disturbance.

6. ACKNOWLEDGMENT

The authors wish to express their appreciation to the Office of Naval Research for the support of research grant N00014-95-1-0539, entitled Integrated Diagnostics. Dr. Peter Schmidt serves as program officer. The authors also wish to express their appreciation to Mr. Andrew Flaherty of Rexnord Corporation for machining the seal rotor, and to Mr. Laurence Thorwart and Mr. David Erich of Pure Carbon Company for providing and machining the graphite stators. This project is also supported in part by a Georgia Tech Foundation Grant, E25-A77, made by Mr. Gilbert Bachman. This support is gratefully acknowledged.

7. REFERENCES

[1] R. F. Salant, A. L. Miller, P. L. Kay, J. Kozlowski, W. E. Kay, and M. C. Algrain, "Development of an Electrically Controlled Mechanical Seal," in *Proc. 11th International Conference on Fluid Sealing*, 1987, pp. 576-595.

[2] A. J. Heilala and A. Kangasneimi, "Adjustment and Control of a Mechanical Seal Against Dry Running and Severe Wear," in *Proc. 11th International Conference on Fluid Sealing*, 1987, pp. 548-575.

[3] I. Etsion, Z. J. Palmor, and N. Harari, "Feasibility Study of a Controlled Mechanical Seal," *Lubrication Engineering*, Vol. 47, No. 8, pp. 621-625, 1991.

[4] P. Wolff and R. F. Salant, "Electronically Controlled Mechanical Seal for Aerospace Applications - Part II: Transient Tests," *Tribology Trans.*, Vol. 38, No. 1, pp. 51-56, 1995.

[5] I. Green, "Gyroscopic and Support Effects on the Steady-State Response of a Noncontacting Flexibly-Mounted Rotor Mechanical face Seal," *ASME Journal of Tribology*, Vol. 111, No. 2, pp. 200-208, 1989.

[6] J. Dayan, M. Zou, and I. Green, "Sensitivity Analysis for the Design and Operation of a Noncontacting Mechanical Face Seal," *IMechE, J. Mech. Eng. Science*, Vol. 214, No. C9, pp. 1207-1218, 2000.

[7] M. Zou, J. Dayan, and I. Green, "Parametric Analysis for Contact Control of a Noncontacting Mechanical Face Seal," in *Proc. of the Vibration, Noise & Structural Dynamics Conf.*, 1999, pp. 493-499.

[8] I. Green, "Gyroscopic and Damping Effects on the Stability of a Noncontacting Flexibly Mounted Rotor Mechanical Face Seal," *Dynamics of Rotating Machinery*, Hemisphere Publishing Company, pp. 153-173, 1990.

[9] M. Zou, J. Dayan, and I. Green, "Dynamic simulation and monitoring of a noncontacting flexibly mounted rotor mechanical face seal," *IMechE, J. Mech. Eng. Science*, Vol. 214, No. C9, pp. 1195-1206, 2000.

[10] A. S. Lee and I. Green, "Higher Harmonic Oscillations in a Noncontacting FMR Mechanical Face Seal Test Rig," *ASME J. Vibration and Acoustics*, Vol. 116, No. 2, pp.161-167, 1994.

[11] A. S. Lee and I. Green, "Physical Modeling and Data Analysis of the Dynamic Response of Flexibly Mounted Rotor Mechanical Seal," *ASME Journal of Tribology*, Vol. 117, No. 1, pp. 130-135, 1995.

[12] A. S. Lee and I. Green, "An Experimental Investigation of the Steady State Response of a noncontacting FMR Mechanical Face Seal," *ASME Journal of Tribology*, Vol. 117, No. 1, pp. 153-159, 1995.

[13] M. Zou and I. Green, "Real-time Condition Monitoring of a Mechanical Face Seal," in *Proc. 24th Leeds-Lyon Symp. On Tribology*, 1997, pp. 423-430.

[14] M. Zou and I. Green, "Clearance Control of a Mechanical Face Seal," STLE Trans, Vol. 42, No. 3, pp. 535-540, 1999.

[15] I. Green, "The Rotor Dynamic Coefficients of Coned-face Mechanical Seals With Inward or Outward Flow," *ASME J. of Tribology*, Vol. 109, No. 1, pp.129-135, 1987.

[16] J. Sehnal, J. Sedy, A. Zobens, and I. Etsion, "Performance of a Coned-Face End Seal With Regard to Energy Conservation," *ASLE Trans*., Vol. 26, No. 4, pp. 415-429, 1983.

[17] I. Etsion and I. Constantinescu, "Experimental Observation of the Dynamic behavior of Noncontacting Coned-face Mechanical Seal," *ASLE Trans*., Vol. 27, No. 3, pp. 263-270, 1984.

[18] M. Zou, J. Dayan, and I. Green, "Feasibility of Contact Elimination of a Mechanical Face Seal Through Clearance Adjustment," *ASME Trans. Gas Turbines &Power*, Vol. 122 No. 3, pp. 478-484, 2000.

[19] S. Shoval, A. Mishan, and J. Dayan, "Odometry and triangulation data fusion for mobile robots environment recognition," *Control Engineering Practice*, No. 6, pp. 1383-1388, 1998.

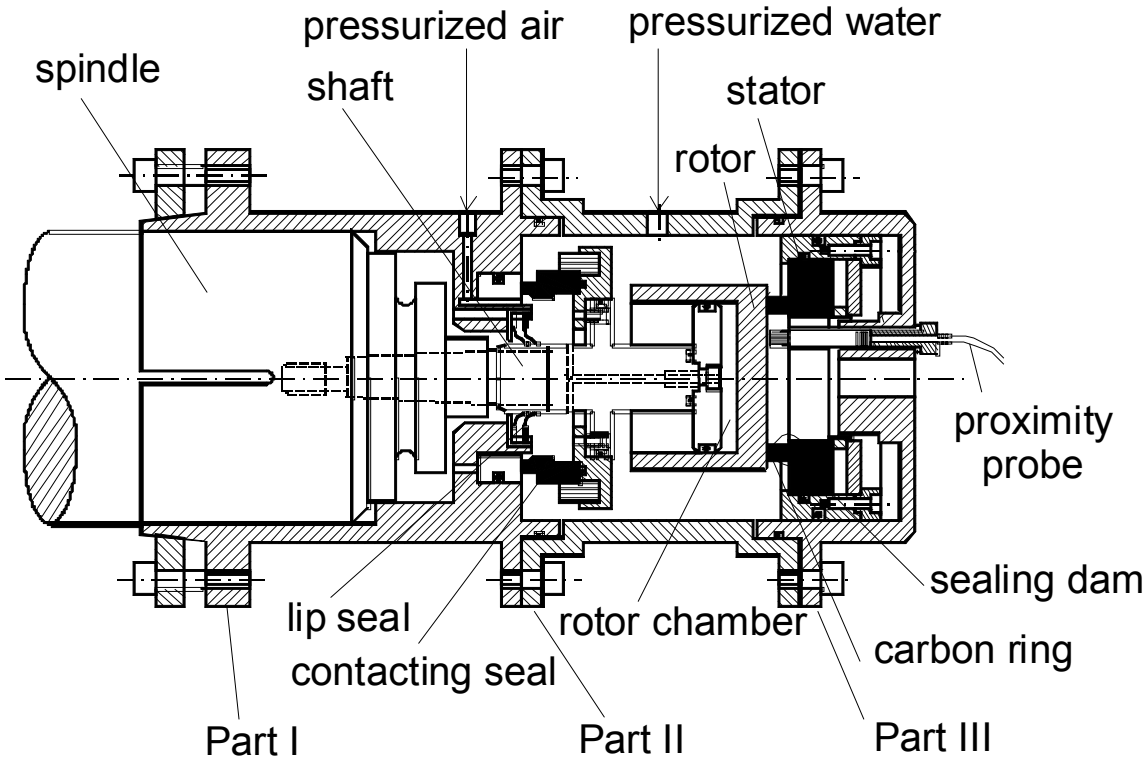

Figure 2: Schematics of the FMR noncontacting mechanical seal assembly